JNS

LABORATORY INVESTIGATION

J Neurosurg 138:1570–1579, 2023

Intranasal delivery of nanoliposomal SN-38 for treatment of diffuse midline glioma

***Takahiro Sasaki, MD, PhD,[1,2] Jun Watanabe, MD, PhD,[3–5] Xingyao He, MS,[1] Hiroaki Katagi, MD, PhD,[1] Amreena Suri, MPH,[3,4] Yukitomo Ishi, MD, PhD,[3,4] Kouki Abe, PhD,[3,4] Manabu Natsumeda, MD, PhD,[5] William H. Frey II, PhD,[6] Peng Zhang, PhD,[1,7] and Rintaro Hashizume, MD, PhD[3,4,7]**

[1]Department of Neurological Surgery, Lou and Jean Malnati Brain Tumor Institute, Northwestern University Feinberg School of Medicine, Chicago, Illinois; [2]Department of Neurological Surgery, Wakayama Medical University, Wakayama, Japan; [3]Department of Pediatrics, Northwestern University Feinberg School of Medicine, Chicago, Illinois; [4]Division of Hematology, Oncology, Neuro-Oncology and Stem Cell Transplantation, Ann & Robert H. Lurie Children's Hospital of Chicago, Illinois; [5]Department of Neurological Surgery, Brain Research Institute, Niigata University, Niigata, Japan; [6]HealthPartners Neuroscience Center, HealthPartners Institute, Saint Paul, Minnesota; and [7]Robert H. Lurie Comprehensive Cancer Center, Northwestern University Feinberg School of Medicine, Chicago, Illinois

OBJECTIVE Diffuse midline gliomas, including diffuse intrinsic pontine gliomas (DIPGs), are among the most malignant and devastating childhood brain cancers. Despite aggressive treatment, nearly all children with these tumors succumb to their disease within 2 years of diagnosis. Due to the anatomical location of the tumors within the pons, surgery is not a treatment option, and distribution of most systematically administered drugs is limited by the blood-brain barrier (BBB). New drug delivery systems that bypass the BBB are desperately needed to improve outcomes of DIPG patients. Intranasal delivery (IND) is a practical and noninvasive drug delivery system that bypasses the BBB and delivers the drugs to the brain through the olfactory and trigeminal neural pathways. In this study, the authors evaluated the efficacy of nanoliposomal (LS) irinotecan (CPT-11) and an active metabolite of CPT-11, 7-ethyl-10-hydroxycamptothecin (SN-38), using IND in DIPG patient-derived xenograft models.

METHODS In vitro responses to LS-CPT-11 and LS-SN-38 in DIPG cells were evaluated with cell viability, colony formation, and apoptosis assays. The cellular uptakes of rhodamine-PE (Rhod)–labeled LS-CPT-11 and LS-SN-38 were analyzed with fluorescence microscopy. Mice bearing DIPG patient-derived xenografts were treated with IND of LS-control (empty liposome), LS-CPT-11, or LS-SN-38 by IND for 4 weeks. In vivo responses were measured for tumor growth by serial bioluminescence imaging and animal subject survival. The concentration of SN-38 in the brainstem tumor administered by IND was determined by liquid chromatography–mass spectrometry (LC-MS). Immunohistochemical analyses of the proliferative and apoptotic responses of in vivo tumor cells were performed with Ki-67 and TUNEL staining.

RESULTS LS-SN-38 inhibited DIPG cell growth and colony formation and increased apoptosis, outperforming LS-CPT-11. Rhod-labeled LS-SN-38 showed intracellular fluorescence signals beginning at 30 minutes and peaking at 24 hours following treatment. LC-MS analysis revealed an SN-38 concentration in the brainstem tumor of 0.66 ± 0.25 ng/ml (5.43% ± 0.31% of serum concentration). IND of LS-SN-38 delayed tumor growth and significantly prolonged animal survival compared with IND of LS-control ($p < 0.0001$) and LS-CPT-11 ($p = 0.003$). IND of LS-SN-38 increased the number of TUNEL-positive cells and decreased the Ki-67–positive cells in the brainstem tumor.

CONCLUSIONS This study demonstrates that IND of LS-SN-38 bypasses the BBB and enables efficient and noninvasive drug delivery to the brainstem tumor, providing a promising therapeutic approach for treating DIPG.

https://thejns.org/doi/abs/10.3171/2022.9.JNS22715

KEYWORDS intranasal delivery; nanoliposome; SN-38; diffuse intrinsic pontine glioma; patient-derived xenograft; oncology

ABBREVIATIONS BBB = blood-brain barrier; CPT-11 = active metabolite of irinotecan; DIPG = diffuse intrinsic pontine glioma; DIPG-007 = HSJD-DIPG-007 cell line; DMG = diffuse midline glioma; IC_{50} = 50% growth inhibition concentration; IND = intranasal delivery; LC-MS = liquid chromatography–mass spectrometry; LS = nanoliposomal; LS-control = empty liposome; PARP = poly (ADP-ribose); PDX = patient-derived xenograft; Rhod = rhodamine-PE [1,2-dioleoyl-*sn*-glycero-3-phosphoethanolamine-*N*-(lissamine rhodamine B sulfonyl)-phospholipid phosphatidylethanolamine]; SN-38 = 7-ethyl-10-hydroxycamptothecin, active metabolite of CPT-11.

SUBMITTED March 25, 2022. **ACCEPTED** September 16, 2022.

INCLUDE WHEN CITING Published online November 11, 2022; DOI: 10.3171/2022.9.JNS22715.

* T.S. and J.W. contributed equally to this work.

©AANS 2023, except where prohibited by US copyright law

Brought to you by CCSS/BINASSS - DEPARTMENTO ADQ | Unauthenticated | Downloaded 06/19/23 04:42 PM UTC

Diffuse midline gliomas (DMGs) are a subtype of high-grade gliomas in the midline area of the brain.[1] Of these, the most malignant and devastating glioma arising in the pons is diffuse intrinsic pontine glioma (DIPG). DIPG is the most rapidly fatal DMG, with a median survival of only 9–12 months from diagnosis.[2,3] The dismal prognosis of these patient is associated with an infiltrative growth pattern in a vital area of the brain (brainstem), which prevents resection and impairs radiotherapy targeting. Moreover, the presence of the blood-brain barrier (BBB) impedes effective distribution of systemically administered chemothrapy.[4] While some systemically administered small molecules reach the brain through the BBB, high doses are required for treatment effects, which can induce substantial toxicity.[4,5] Local drug delivery to the brain tumor using intraventricular or intraparenchymal injections (e.g., convection-enhanced delivery) is invasive, has substantial surgical risks, and is expensive.[6–8] Additional limitations of these local drug delivery methods are insufficient parenchymal penetration due to slow diffusion from the infusion site and rapid CSF flow and absorption.[9–11] The development of new therapeutic approaches that facilitate drug delivery while bypassing the BBB and eliminating the surgical risks of direct drug delivery is a great need to improving outcomes for DIPG patients.

Intranasal delivery (IND) is a practical and noninvasive method of drug delivery to the brain that bypasses the BBB through the unique anatomical connections between the nasal mucosa and brain.[4,12–15] Drugs administered by IND are distributed within minutes to the supratentorial brain along with the olfactory nerve and to the infratentorial brain along with the trigeminal nerve. These extracellular pathways through perineural and perivascular channels deliver the drugs to the brain without using any receptors or relying on axonal transportation.[13] Other benefits of IND are the avoidance of drug metabolism in the liver, which reduces unwanted systemic toxicity, and convenient self-administration for patients, which is important when multiple doses are required in treating a brain tumor. IND is a potential alternative to systemic (intravenous) or direct invasive (intraventricular, convection-enhanced delivery) drug delivery for the treatment of brain tumors.[11,12,14] This technique has been used for delivering many chemotherapeutic agents and has shown promising results in the treatment of human brain disorders and rodent brain tumor without systemic toxicity. IND of temozolomide (NCT04091503) and perillyl alcohol (POH; NCT02704858)[16–18] has been tested in clinical trials for adult patients with glioblastoma. We have previously shown that IND of GRN163, an oligonucleotide telomerase inhibitor, inhibited intracranial tumor growth and prolonged the survival of rats bearing orthotopic human brain tumors without harming the healthy normal brain tissues.[19,20]

The effectiveness of IND for certain therapeutic roles can be increased by using nanoliposomal (LS) drug carriers, which provide stable encapsulation for the agents, improving solubility and bioavailability.[21–23] LS formulations provide greater brain penetration due to the liposome-mediated protection of the entrapped agents from enzymatic degradation and clearance from the brain.[24,25] We have recently shown the antitumor activity of an LS formulation of irinotecan (CPT-11), an inhibitor of DNA topoisomerase I, by IND in human brainstem xenograft models.[26] IND of LS-CPT-11 had an increased survival benefit relative to IND of LS-control (empty liposome). However, IND of LS-CPT-11 showed only modest activity in vivo due to the limitation of hepatic metabolism of CPT-11 to its active metabolite SN-38 (7-ethyl-10-hydroxycamptothecin), which exerts 1000 times stronger cytotoxic activity than CPT-11.[27,28] LS-SN-38 largely increases the solubility of SN-38, of which the low solubility is one of the major hurdles to its clinical application. In addition, compared with its prodrug version LS-CPT-11, LS-SN-38 has an improved pharmacodynamic profile, in parallel with safety and efficacy profiles.[29,30] In the present study, we utilized LS-SN-38 as a model drug to establish an efficient and noninvasive drug delivery approach, IND, for treating DIPG using an intracranial patient-derived xenograft (PDX) model.

Methods

Cell Sources

The primary human DIPG cell line SF8628 was obtained from the University of California, San Francisco (UCSF) Medical Center. The SF8628 cell line was established from a surgical specimen and modified to express firefly luciferase for in vivo bioluminescence imaging.[8,26,31,32] The HSJD-DIPG-007 cell line (DIPG-007) was a kind gift from Dr. Angel Montero Carcaboso (Hospital Sant Joan de Déu, Barcelona, Spain). SF8628 cells were cultured in DMEM supplemented with 10% fetal bovine serum (FBS) and nonessential amino acids (11140-050) from Thermo Fisher. DIPG-007 cells were grown adherently in tumor stem medium base consisting of neurobasal-A medium, DMEM/F-12 medium, HEPES buffer, sodium pyruvate, MEM nonessential amino acids, GlutaMAX-I supplement, antibiotic-antimycotic, B-27 supplement minus vitamin A from Thermo Fisher, epidermal growth factor and fibroblast growth factor (Shenandoah Biotech), platelet-derived growth factors A and B (Shenandoah Biotech), 0.2% heparin (STEMCELL Technologies), and 5% FBS. Cell sources were authenticated by short tandem repeat profiling using the Powerplex 16HS system (Promega). Freedom from *Mycoplasma* infection was verified with the *Mycoplasma* detection kit (Invitrogen).

LS Agents

LS-control (empty liposome), LS-CPT-11, and LS-SN-38 were generated using a thin film rehydration method at a dose of 1 mg/ml for each drug. Briefly, 1,2-dioleoyl-*sn*-glycero-3-phosphocholine, 1′,3′-bis[1,2-dioleoyl-*sn*-glycero-3-phospho]-glycerol, cholesterol, and 1,2-distearoyl-*sn*-glycero-3-phosphoethanolamine-*N*-[methoxy(polyethylene glycol)-2000] were mixed in chloroform at a molar ratio of 55:10:30:5. Drugs dissolved in chloroform/methanol (4:1) were added into the mixture of lipids at a lipid/drug molar ratio of 10:1. To track the distribution of liposomes, LS formulations contained 1,2-dioleoyl-*sn*-glycero-3-phosphoethanolamine-*N*-(lissamine

Brought to you by CCSS/BINASSS - DEPARTMENTO ADQ | Unauthenticated | Downloaded 06/19/23 04:42 PM UTC

rhodamine B sulfonyl)-phospholipid phosphatidylethanolamine (Rhod) at a molar ratio of 0.5%. Chloroform was evaporated using a rotary evaporator (Buchi), and dried by vacuum for 4 hours. Dulbecco's phosphate-buffered saline was added to the formed thin film for 4 hours for hydration. The thin film was suspended by vortex to obtain an opaque solution. The solution was further homogenized using an ultrasonic homogenizer (BioLogics) on ice.

Cell Viability and Colony Formation Assays

Cell viability was analyzed using the CellTiter 96 AQ_{ueous} One Solution cell proliferation assay (Promega). Tumor cells were seeded in 96-well plates, at 2000 cells per well, and cultured in the presence of 0–2.0 μM free drugs and LS-CPT-11 or LS-SN-38 for 72 hours, with quadruplicate samples for each incubation condition. The 50% growth inhibition concentration (IC_{50}) values were calculated using nonlinear least-squares curve fitting. Inhibitor proliferation effects were determined using a cell viability assay on days 1, 2, 3, 4, and 5 in the presence of LS-control or LS-CPT-11 (5 nM) and LS-SN-38 (5 nM), with triplicate samples for each incubation condition. For colony formation assays, 300–1000 cells were seeded in 60-mm plates (or 6-well plates) and then treated with administration of LS-control or IC_{50} values of LS-CPT-11 or LS-SN-38 for 72 hours. After 2 weeks, cells were stained with 0.05% crystal violet and colonies were counted. Values shown are the averages (means ± standard deviations) from triplicate samples for each condition.

Apoptosis Assay

To evaluate whether treatments induced apoptosis, tumor cells were treated with LS-control, LS-CPT-11, or LS-SN-38 for 72 hours. Cells were stained with propidium iodide (PI) staining solution and fluorescein isothiocyanate (FITC)–annexin V by use of the BD Pharmingen FITC Annexin V Apoptosis Detection Kit I (BD Biosciences) and sorted using flow cytometry (BD LSRFortessa Analyzer cytometer). The ratio of apoptotic cells (annexin V positive and annexin V+PI double positive) was calculated using FlowJo software (version 10.5).

In Vitro Cellular Uptake and Distribution

SF8628 cells were treated with Rhod-labeled LS-SN-38 and LS-CPT-11 in 6-well plates. The cells were imaged with a fluorescent microscope at 0.5, 3, 6, and 24 hours after treatment for the evaluation of cellular uptake and intracellular localization.

Xenograft Models

Six-week-old female athymic mice (rnu/rnu genotype, BALB/c background) were obtained from Envigo and maintained under pathogen-free conditions. Luciferase-modified SF8628 cells were implanted into the pons of athymic mice as described previously.[8,26,31,32] Briefly, a 100,000-cell/μl suspension was injected into the pontine tegmentum at a depth of 5 mm from the inner base of the skull using a 26-gauge Hamilton syringe (Hamilton Company). All procedures were performed under sterile conditions.

All animal experiments were approved by the Northwestern University Institutional Animal Care and Use Committee (IACUC).

Intranasal Delivery

IND was conducted as previously described.[19,26] Briefly, mice were anesthetized with 2.5% isoflurane and placed in a supine position in an anesthesia chamber. Drops (3 μl) containing LS-control, LS-CPT-11, and LS-SN-38 were administered with a p10 pipette tip every 2 minutes into each naris for a total volume of 30 μL (30 μg) of an LS drug each session. Mice were kept in a supine position during the administration and remained in this position for 10 minutes postadministration to optimize absorption through the nasal mucosa. This administration method can deposit the agents consistently into the olfactory epithelium without respiratory distress.

Analysis of Drug Concentration in the Brainstem Tumor

Athymic mice bearing orthotopic (i.e., brainstem) DIPG xenografts were treated with IND of LS-CPT-11 or LS-SN-38 for 5 days,[19,26] and the brains were resected after the mice were euthanized, within 3 hours following completion of the treatment. The brainstem tumors and the normal brains were dissected, and serum samples were collected by cardiac puncture and snap frozen in the liquid nitrogen. CPT-11 and SN-38 were extracted from homogenized tissue and serum, and the drug concentrations were determined by liquid chromatography–mass spectrometry (LC-MS) analysis (Shimadzu VP Series 10 System, Integrated Analytical Systems).

In Vivo Therapy Response Study

SF8628 cells (100,000 cells/μl) were implanted into the pons as described above (day 0). Mice were randomly assigned to three treatment groups: 1) IND LS-control (n = 8), 2) IND LS-CPT-11 (n = 8), and 3) IND LS-SN-38 (n = 8), and the treatment was initiated on day 23 and continued for 5 days a week for 4 weeks. Tumor growth and response to therapy were monitored weekly by bioluminescence imaging. Mice were observed daily and euthanized when in a moribund condition, which was defined by an irreversible neurological deficit or a body condition score less than 2.

Immunohistochemistry

Mice were euthanized at 3 hours following completion of the last treatment. Resected brains from mice (n = 3) were processed for paraformaldehyde-fixed and paraffin-embedded sections (10 μm) for immunohistochemical analysis. These sections were stained with H&E, anti–Ki-67 (2 μg/ml; Ventana Inc.), TUNEL (DeadEnd Colorimetric TUNEL system, Promega), and anticleaved–poly (ADP-ribose) (PARP) and anticleaved–caspase 3 (2 μg/ml; Cell Signaling).

Statistical Analysis

Animal survival rates were analyzed using the Kaplan-Meier method (GraphPad Prism software version 7.0)

Brought to you by CCSS/BINASSS - DEPARTMENTO ADQ | Unauthenticated | Downloaded 06/19/23 04:42 PM UTC

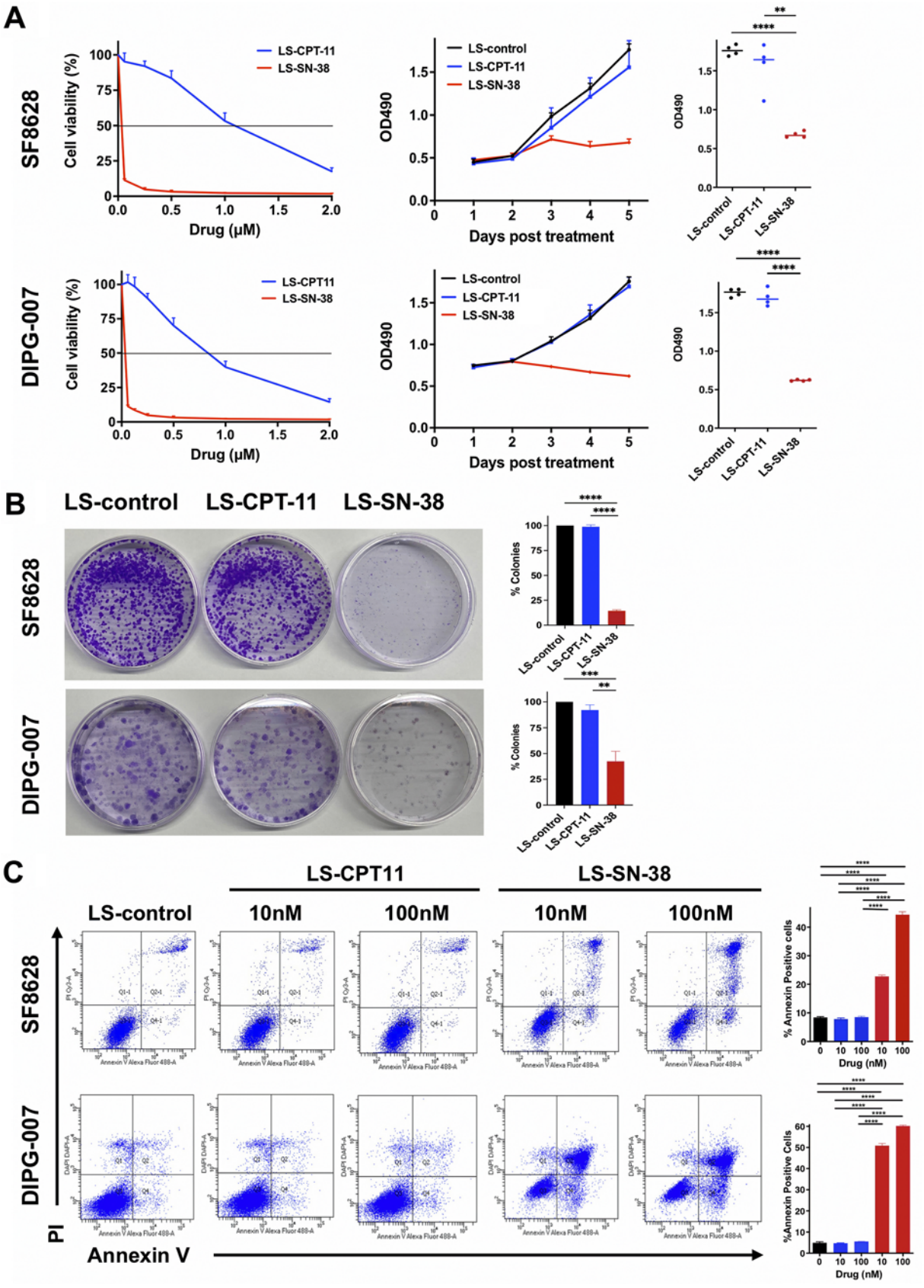

FIG. 1. Cytotoxic activity of LS-CPT-11 and LS-SN-38 in vitro. **A:** DIPG cells (*upper*: SF8628, *lower*: DIPG-007) are treated with LS-CPT-11 and LS-SN-38. *Left*: Cell viability was determined by MTS assay after 72 hours. **FIG. 1.** (*continued*) →

Brought to you by CCSS/BINASSS - DEPARTMENTO ADQ | Unauthenticated | Downloaded 06/19/23 04:42 PM UTC

FIG. 1. Values shown are the average (mean ± SD) from quadruplicate samples for each condition. *Center*: Cell growth plot showing OD 490 values as the proliferation response to LS-CPT-11 and LS-SN-38 treatment of DIPG cells at each time point. Values shown are the average (mean ± SD) from duplicate or triplicate samples for each condition. *Right*: Dot plot representation of OD 490 values on day 5. Statistical analysis was performed using a two-tailed unpaired t-test: ****p < 0.0001; SF8628, **p = 0.0014. **B:** Colony-forming effect on SF8627 (*upper*) and DIPG-007 (*lower*) cells treated with LS-control (empty liposomes), LS-CPT-11, and LS-SN-38. *Right*: Bar graph representation of colony numbers in each cell line. Values shown are the average (mean ± SD) from triplicate samples for each condition. Unpaired t-test values for comparisons between each treatment group: ****p < 0.0001; DIPG-007, ***p = 0.0005, **p = 0.0015. **C:** Annexin V flow cytometry analysis of apoptosis effects. SF8628 (*upper*) and DIPG-007 (*lower*) cells were treated with LS-control, LS-CPT-11 (10 nM, 100 nM), or LS-SN-38 (10 nM, 100 nM). The cells were collected and treated with Alexa Fluor 488 annexin V and flow sorted. *Right*: Bar graph representation of annexin V–positive cell numbers. Values shown are the average (mean ± SD) from quadruplicate samples for each incubation condition. One-way ANOVA values for comparisons of each treatment: ****p < 0.0001.

and estimated by use of a log-rank test. For other analyses, a two-tailed unpaired Student t-test and one-way ANOVA with Tukey's multiple comparisons were applied using Prism software.

Results

Effects of LS-SN-38 on Cell Proliferation and Apoptosis in DIPG Cells

We first examined in vitro responses to free CPT-11 and free SN-38 and to LS-CPT-11 and LS-SN-38 in two DIPG cell lines (SF8628 and DIPG-007). LS-CPT-11 and LS-SN-38 showed greater inhibition of DIPG cell growth than free drugs (IC_{50} values of LS drugs vs free drugs: 1.06 vs 2.00 μM for CPT-11 and 0.145 vs 0.388 μM for SN-38 in SF8628 cells; 0.79 vs 1.31 μM for CPT-11 and 0.227 vs 0.515 μM for SN-38 in DIPG-007 cells; Supplementary Fig. S1). These results suggest that the liposomal formulation improves drug delivery into the cell, resulting in increased cytotoxicity compared with the nonliposomal formulation. LS-SN-38 inhibited the growth of DIPG cells in a dose-dependent manner, outperforming LS-CPT-11 (IC_{50} values of LS-SN-38 vs LS-CPT-11: 5 nM vs 1 μM in SF8628 cells and 4 nM vs 0.7 μM in DIPG-007 cells; Fig. 1A). At the IC_{50} value, LS-SN-38 significantly reduced DIPG cell growth relative to the LS-control ($p < 0.0001$

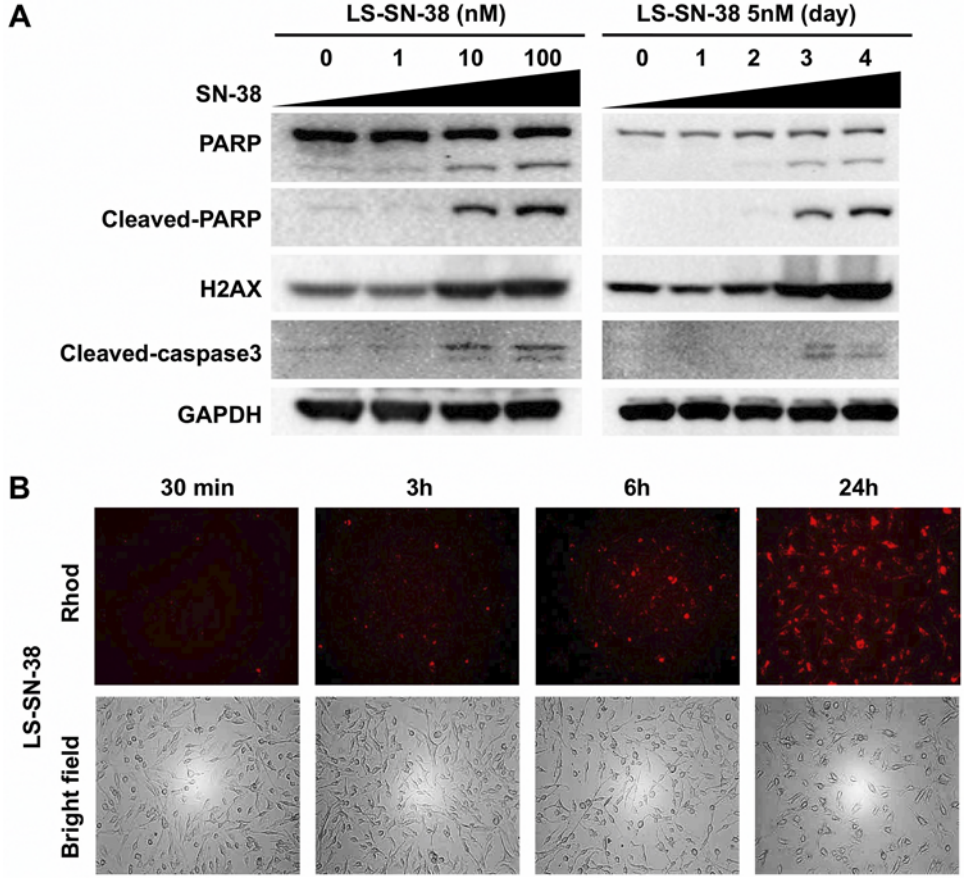

FIG. 2. Effects of LS-SN-38 on the expression of apoptosis and DNA damage markers and cellular uptake. **A:** Western blotting results showing expression of PARP, cleaved PARP, H2AX, cleaved caspase 3, and GAPDH in SF8628 DIPG cells treated with LS-SN-38. **B:** Fluorescent microscopic evaluation of cellular uptake and intracellular localization of LS-SN-38 in DIPG cells. Single cells of SF8628 were seeded into 6-well plates and were treated with Rhod-labeled LS-SN-38. DIPG cells were imaged with a fluorescent microscope at 30 minutes and 3, 6, and 24 hours after treatment.

Brought to you by CCSS/BINASSS - DEPARTMENTO ADQ | Unauthenticated | Downloaded 06/19/23 04:42 PM UTC

TABLE 1. SN-38 concentration in serum and brainstem tumor after IND of LS-CPT-11 and LS-SN-38

	SN-38 Concentration (ng/ml)	
	LS-CPT-11	LS-SN-38
Serum	30.3 ± 10.9	12.8 ± 3.3
Brainstem tumor	0.34 ± 0.12	0.66 ± 0.25

Values are reported as mean ± SD.

in both SF8628 and DIPG-007 cells on day 5) and LS-CPT-11 ($p = 0.0014$ vs $p < 0.0001$ for SF8628 vs DIPG-007 on day 5; Fig. 1A). LS-SN-38 also inhibited colony formation relative to both the LS-control ($p < 0.0001$ vs $p = 0.0005$ for SF8628 vs DIPG-007 cells) and LS-CPT-11 ($p < 0.0001$ vs $p = 0.0015$ for DIPG-007 cells; Fig. 1B). LS-SN-38 increased apoptosis (annexin V–positive cells: 8.4% with LS-control vs 8.5% with 100 nM LS-CPT-11 vs 44.3% with 100 nM LS-SN-38 in SF8628 cells and 4.9% with LS-control vs 5.5% with 100 nM LS-CPT-11 vs 60.2% with 100 nM LS-SN-38 in DIPG-700 cells; Fig. 1C). LS-SN-38 also increased the expression of apoptosis markers (cleaved PARP, caspase 3) and DNA damage marker γH2AX in a dose- and time-dependent manner (Fig. 2A). To determine the cellular distribution of LS-SN-38, we treated DIPG cells with Rhod-labeled LS-SN-38 and performed imaging with a fluorescent microscope at 30 minutes and 3, 6, and 24 hours after treatment. Fluorescence intensity in SF8628 cells was detected at 30 minutes and largely increased in a time-dependent manner, reaching a peak at 24 hours following treatment (Fig. 2B).

Concentration of SN-38 in the Brainstem Tumor Following IND of LS-CPT-11 and LS-SN-38

To evaluate whether liposomal encapsulation provides increased nasal penetration and brain distribution of the anticancer agents, we performed 5 days of IND administration of LS-CPT-11 and LS-SN-38 into the mice bearing orthotopic DIPG xenografts and then euthanized the mice 3 hours after completion of the IND treatment. LC-MS analysis of tissue extracts revealed higher concentrations of SN-38 in brainstem tumors in the mice treated with LS-SN-38 (0.66 ± 0.25 ng/ml, 5.43% ± 0.31% serum concentration) than in the mice treated with LS-CPT-11 (0.34 ± 0.12 ng/ml, 1.24% ± 0.67% serum concentration; Table 1). These results may indicate that the drug distribution profile of LS-SN-38 in the brainstem tumor with IND administration was more favorable than that for LS-CPT-11.

IND of LS-CPT-11 and LS-SN-38 in DIPG PDX Models

The promising biological effects of LS-SN-38 in vitro encouraged us to further evaluate the potency of LS-SN-38 by IND to suppress tumor growth and increase survival of mice bearing orthotopic DIPG PDX models. We first assessed in vivo toxicity by monitoring weight loss (> 15% of initial weight), body condition, and inability to move in the mice treated with LS-control, LS-CPT-11, and LS-SN-38. We found that the mean body weight of all the treatment groups increased following completion of treatments, results comparable to those of the control

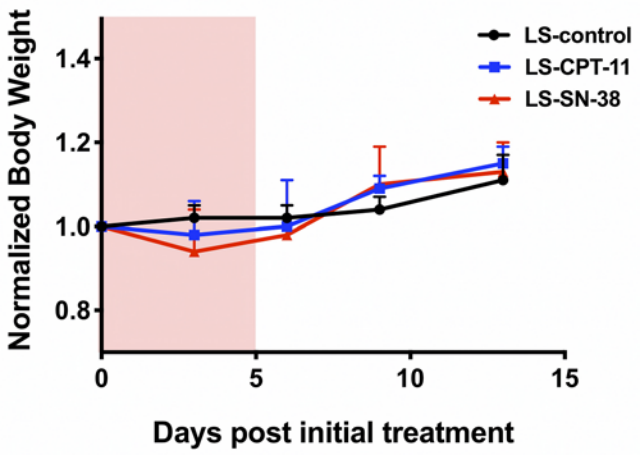

FIG. 3. Effect of IND of LS-CPT-11 and LS-SN-38 on body weights of mice. Three mice were treated with IND of LS-CPT-11 or LS-SN-38 for 5 days (*orange area*). The mean (*symbols*) and standard deviation (*error bars*) values of normalized body weights at day 0 before treatment are shown.

group (Fig. 3). No treatment-related toxicity was detected. To evaluate the in vivo antitumor activity of LS-SN-38, we treated mice bearing orthotopic DIPG xenografts with IND of LS-CPT-11 or LS-SN-38 for 20 days. IND of LS-SN-38 inhibited tumor growth ($p = 0.004$; Fig. 4A) and significantly increased survival of the mice with DIPG xenograft compared with the mice treated with LS-control ($p < 0.0001$) and LS-CPT-11 ($p = 0.003$; Fig. 4B). Two mice in each treatment group were euthanized following completion of treatment. Brainstem tumors from the mice were analyzed for tumor cell proliferation (Ki-67 staining) and apoptosis (TUNEL, cleaved PARP, and cleaved caspase 3 staining). Immunohistochemical analysis of brainstem tumors by Ki-67 staining revealed that IND of LS-SN-38 decreased the number of Ki-67–positive cells compared with IND of LS-control ($p = 0.0006$) and LS-CPT-11 ($p = 0.015$; Fig. 4C). Staining with TUNEL, cleaved PARP, and cleaved caspase 3 showed that IND of LS-SN-38 increased positive cells compared with IND of LS-control (TUNEL: $p = 0.0002$, Fig. 4C; cleaved PARP: $p = 0.0048$; cleaved caspase 3: $p = 0.0127$, Supplementary Fig. S2) or LS-CPT-11 (TUNEL: $p = 0.0023$, Fig. 4C; cleaved PARP: $p = 0.0106$, cleaved caspase 3: $p = 0.0182$, Supplementary Fig. S2).

Discussion

Developing a new drug delivery system that bypasses the BBB is a potential strategy for the treatment of children with DIPG. IND has been shown to provide effective and noninvasive drug delivery of chemotherapy to the brain for treating patients with CNS disorders, including brain tumor.[18] IND has even been shown to deliver therapeutic stem cells to the targeted brain tumor in animal models.[33–38] IND of temozolomide (NCT04091503) and POH (NCT02704858)[16–18] has been used in clinical trials for adult glioblastoma. The antitumor activity of POH was convincingly established in preclinical models.[16,17] The administration route of POH was switched to IND from the

Brought to you by CCSS/BINASSS - DEPARTMENTO ADQ | Unauthenticated | Downloaded 06/19/23 04:42 PM UTC

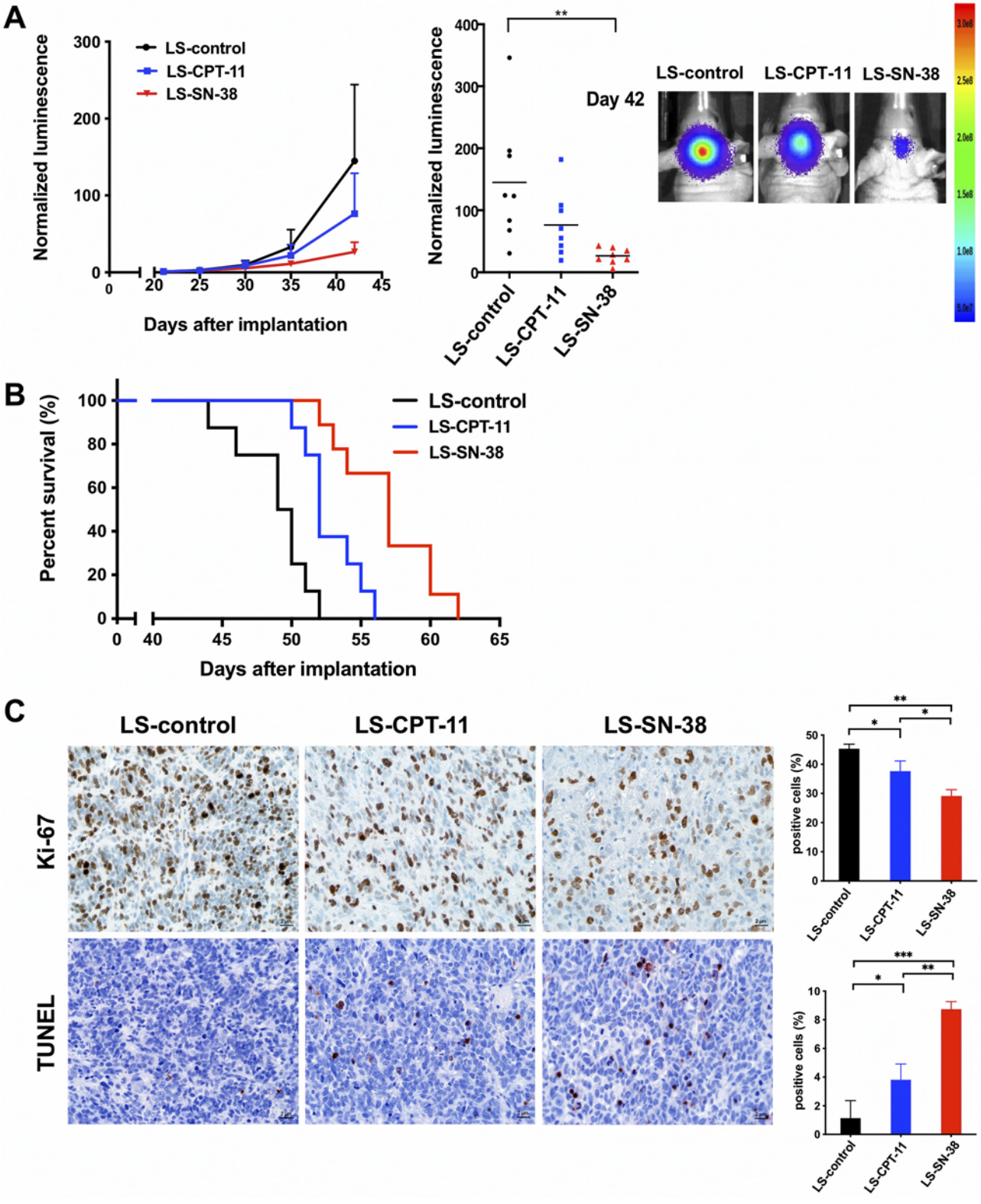

FIG. 4. Antitumor effect of IND of LS-CPT-11 and LS-SN-38 on tumor growth in DIPG xenografts. Mice with SF8628 intracranial tumor were randomized to three treatment groups: LS-control, LS-CPT-11, and LS-SN-38. **A:** Growth plots (*left*) of tumor bioluminescence in each treatment group. Tumor bioluminescence values show the mean (*symbols*) and standard deviation (*error bars*) values for normalized against bioluminescence values obtained at day 21 posttumor cell injection. Dot plot (*middle*) representation of tumor bioluminescence values in mice at day 42 posttumor cell injection. *Horizontal bars* indicate the mean value for each treatment group. Representative tumor bioluminescence overlay images (*right*) showing relative bioluminescence intensities in each treatment group. **B:** Corresponding survival analysis for each experiment. **C:** Immunohistochemical analysis of DIPG xenografts treated with IND of LS-CPT-11 or LS-SN-38. **FIG. 4.** (*continued*) →

Brought to you by CCSS/BINASSS - DEPARTMENTO ADQ | Unauthenticated | Downloaded 06/19/23 04:42 PM UTC

FIG. 4. Images of representative Ki-67 and TUNEL staining of intracranial tumor from mice euthanized at the end of treatment. The mean and standard deviation (*error bars*) values represent the average number of positive cells in three high-powered fields for each tumor. Statistical analysis was performed with ANOVA with Tukey multiple comparisons. Ki-67: LS-control versus LS-CPT-11, *p = 0.0231; LS-control versus LS-SN-38, ***p = 0.0006; LS-CPT-11 versus LS-SN-38, *p = 0.0155. TUNEL: LS-control versus LS-CPT-11, *p = 0.0393; LS-control versus LS-SN-38, ***p = 0.0002; LS-CPT-11 versus LS-SN-38, **p = 0.0023.

oral route because clinical trials of oral POH failed due to severe gastrointestinal side effects.[18]

CPT-11 is clinically used against brain tumors and other cancers by intravenous infusion; however, severe systemic side effects including diarrhea are also common in patients treated with CPT-11.[27,28] We have previously shown that IND of LS-CPT-11 increased the survival benefit without toxicity in human brainstem xenograft models,[26] while IND of LS-CPT-11 has modest activity at best in vivo due to the limitation of hepatic metabolism to its active metabolite SN-38.[27,28] SN-38 has a potent cytotoxic activity; however, the poor solubility of SN-38 is a problem for clinical use.[32] IND of LS-SN-38 can solve both problems, the systemic adverse effects and the poor solubility, in parallel with avoidance of hepatic metabolism when compared with the prodrug version, LS-CPT-11.

Indeed, our LC-MS analysis revealed higher concentrations of SN-38 at the brainstem tumors in the mice treated with LS-SN-38 than in the mice treated with LS-CPT-11 (Table 1). To further enhance the drug distribution to a brainstem tumor mass, an active targeting strategy will be applied to our liposomal formulation, which depends on the surface modification of liposomes with ligand motifs that have high binding affinity with overexpressed receptors on tumor cells.[39] IND is often facilitated by deposition of drug in the upper area of the nasal cavity (i.e., the olfactory region).[21] However, in order to target the brainstem, it will likely be better to administer the liposomal formulation to the respiratory epithelium, which is rich in trigeminal nerve endings.[40] One preclinical study, for example, has shown that a lipid nanoparticle formulation of the neurotrophin growth differentiation factor 5 resulted in more efficient delivery to the midbrain, pons, medulla, and cerebellum, with much lower administration to the olfactory epithelium and olfactory bulb.[41] For that reason, we will test the nasal spray devices that target delivery to the respiratory epithelium and most effectively transmit the agents to the brainstem tumor through the trigeminal neural pathway. Whenever one adds formulation components to therapeutics to be administered with IND, it is important to consider the possibility that one or more of the formulation components will also be delivered into the brain and to assess potential impacts of such components on the olfactory and trigeminal nerves and brain.

Because IND of liposomal SN-38 does result in significant delivery to the bloodstream (Table 1), we intend to assess the use of a nasal vasoconstrictor to reduce systemic exposure, as this has been shown to work for other intranasal therapeutics.[42] While a high concentration of SN-38 was detected in the serum, all mice tolerated IND of LS-SN-38 (Fig. 3). We previously reported that a liposomal formulation of CPT-11, administered intranasally, delivered both the drug and liposomal components to the brainstem tumor without any obvious adverse side effects.[26] In addition, histological evaluation after IND showed no apparent damage of nasal mucosa such as congestion, edema, epithelial sloughing, necrosis, or hemorrhage associated with the administration of plain liposomes in human volunteers[43] or calcitonin-loaded liposomes in rats.[44]

Our in vivo efficacy study provides evidence that IND of LS-SN-38 inhibited tumor growth and increased the survival benefit in DIPG xenograft models when compared with IND of LS-CPT-11 (Fig. 4). Furthermore, treatment with IND of LS-SN-38 promotes apoptosis and cell death (Fig. 4). Taking all of the results, our observations indicate that IND of LS-SN-38 is a promising therapeutic strategy for treating DIPG in a preclinical model and support further development of IND of LS-SN-38 as a potential therapy for DIPG patients.

Conclusions

This study demonstrates that IND of LS-SN-38 enables noninvasive, therapeutically effective brain delivery of SN-38 in a DIPG xenograft model and provides preclinical evidence in support of the use of LS-SN-38 administered by IND for the treatment of children with this deadly brain cancer.

Acknowledgments

We thank Dr. Angel Montero Carcaboso (Hospital Sant Joan de Déu, Barcelona, Spain) for use of the HSJD-DIPG-007 cell line. Histological analysis was provided by the Mouse Histology and Phenotyping Laboratory at Northwestern University. This work was supported by the US National Institutes of Health (R01NS126513 to R.H.), Japanese Society for Promotion of Science (JSPS) Overseas Research Fellowships (J.W.), Alex's Lemonade Stand Foundation (R.H.), St. Baldrick's Foundation (R.H.), Rally Foundation (R.H.), Segal Family Foundation (R.H.), The Cure Starts Now Foundation (R.H.), and the Pediatric Cancer Research Foundation (R.H.).

References

1. Louis DN, Perry A, Reifenberger G, et al. The 2016 World Health Organization Classification of Tumors of the Central Nervous System: a summary. *Acta Neuropathol*. 2016;131(6):803-820.
2. Robison NJ, Kieran MW. Diffuse intrinsic pontine glioma: a reassessment. *J Neurooncol*. 2014;119(1):7-15.
3. Clymer J, Kieran MW. The integration of biology into the treatment of diffuse intrinsic pontine glioma: a review of the North American clinical trial perspective. *Front Oncol*. 2018;8(8):169.
4. Haumann R, Videira JC, Kaspers GJL, van Vuurden DG, Hulleman E. Overview of current drug delivery methods across the blood-brain barrier for the treatment of primary brain tumors. *CNS Drugs*. 2020;34(11):1121-1131.
5. van Tellingen O, Yetkin-Arik B, de Gooijer MC, Wesseling P, Wurdinger T, de Vries HE. Overcoming the blood-brain tumor barrier for effective glioblastoma treatment. *Drug Resist Updat*. 2015;19:1-12.
6. Bobo RH, Laske DW, Akbasak A, Morrison PF, Dedrick RL, Oldfield EH. Convection-enhanced delivery of macromol-

Brought to you by CCSS/BINASSS - DEPARTMENTO ADQ | Unauthenticated | Downloaded 06/19/23 04:42 PM UTC

ecules in the brain. *Proc Natl Acad Sci U S A*. 1994;91(6):2076-2080.
7. Pardridge WM. Blood-brain barrier drug targeting: the future of brain drug development. *Mol Interv*. 2003;3(2):90-105, 51.
8. Sasaki T, Katagi H, Goldman S, Becher OJ, Hashizume R. Convection-enhanced delivery of enhancer of zeste homolog-2 (EZH2) inhibitor for the treatment of diffuse intrinsic pontine glioma. *Neurosurgery*. 2020;87(6):E680-E688.
9. Kawakami K, Kawakami M, Kioi M, Husain SR, Puri RK. Distribution kinetics of targeted cytotoxin in glioma by bolus or convection-enhanced delivery in a murine model. *J Neurosurg*. 2004;101(6):1004-1011.
10. Mamot C, Nguyen JB, Pourdehnad M, et al. Extensive distribution of liposomes in rodent brains and brain tumors following convection-enhanced delivery. *J Neurooncol*. 2004;68(1):1-9.
11. Sandberg DI, Edgar MA, Souweidane MM. Convection-enhanced delivery into the rat brainstem. *J Neurosurg*. 2002;96(5):885-891.
12. Dhuria SV, Hanson LR, Frey WH II. Intranasal delivery to the central nervous system: mechanisms and experimental considerations. *J Pharm Sci*. 2010;99(4):1654-1673.
13. Chen XQ, Fawcett JR, Rahman YE, Ala TA, Frey WH II. Delivery of nerve growth factor to the brain via the olfactory pathway. *J Alzheimers Dis*. 1998;1(1):35-44.
14. Crowe TP, Greenlee MHW, Kanthasamy AG, Hsu WH. Mechanism of intranasal drug delivery directly to the brain. *Life Sci*. 2018;195(195):44-52.
15. Lochhead JJ, Davis TP. Perivascular and perineural pathways involved in brain delivery and distribution of drugs after intranasal administration. *Pharmaceutics*. 2019;11(11):598.
16. Chen TC, Fonseca CO, Schönthal AH. Preclinical development and clinical use of perillyl alcohol for chemoprevention and cancer therapy. *Am J Cancer Res*. 2015;5(5):1580-1593.
17. Chen TC, da Fonseca CO, Schönthal AH. Intranasal perillyl alcohol for glioma therapy: molecular mechanisms and clinical development. *Int J Mol Sci*. 2018;19(12):3905.
18. Schönthal AH, Peereboom DM, Wagle N, et al. Phase I trial of intranasal NEO100, highly purified perillyl alcohol, in adult patients with recurrent glioblastoma. *Neurooncol Adv*. 2021;12;3(1):vdab005.
19. Hashizume R, Ozawa T, Gryaznov SM, et al. New therapeutic approach for brain tumors: intranasal delivery of telomerase inhibitor GRN163. *Neuro Oncol*. 2008;10(2):112-120.
20. Hashizume R, Gupta N. Telomerase inhibitors for the treatment of brain tumors and the potential of intranasal delivery. *Curr Opin Mol Ther*. 2010;12(2):168-175.
21. Alshweiat A, Ambrus R, Csoka I. Intranasal nanoparticulate systems as alternative route of drug delivery. *Curr Med Chem*. 2019;26(35):6459-6492.
22. Hong SS, Oh KT, Choi HG, Lim SJ. Liposomal formulations for nose-to-brain delivery: recent advances and future perspectives. *Pharmaceutics*. 2019;11(10):540.
23. Gabizon A, Shmeeda H, Barenholz Y. Pharmacokinetics of pegylated liposomal doxorubicin: review of animal and human studies. *Clin Pharmacokinet*. 2003;42(5):419-436.
24. Arumugam K, Subramanian GS, Mallayasamy SR, Averineni RK, Reddy MS, Udupa N. A study of rivastigmine liposomes for delivery into the brain through intranasal route. *Acta Pharm*. 2008;58(3):287-297.
25. Migliore MM, Vyas TK, Campbell RB, Amiji MM, Waszczak BL. Brain delivery of proteins by the intranasal route of administration: a comparison of cationic liposomes versus aqueous solution formulations. *J Pharm Sci*. 2010;99(4):1745-1761.
26. Louis N, Liu S, He X, et al. New therapeutic approaches for brainstem tumors: a comparison of delivery routes using LS irinotecan in an animal model. *J Neurooncol*. 2018;136(3):475-484.
27. Ramesh M, Ahlawat P, Srinivas NR. Irinotecan and its active metabolite, SN-38: review of bioanalytical methods and recent update from clinical pharmacology perspectives. *Biomed Chromatogr*. 2010;24(1):104-123.
28. Si J, Zhao X, Gao S, Huang D, Sui M. Advances in delivery of Irinotecan (CPT-11) active metabolite 7-ethyl-10-hydroxy-camptothecin. *Int J Pharm*. 2019;568(568):118499.
29. Bulbake U, Doppalapudi S, Kommineni N, Khan W. Liposomal formulations in clinical use: an updated review. *Pharmaceutics*. 2017;9(2):12.
30. Fang YP, Chuang CH, Wu YJ, Lin HC, Lu YC. SN38-loaded <100 nm targeted liposomes for improving poor solubility and minimizing burst release and toxicity: in vitro and in vivo study. *Int J Nanomedicine*. 2018;13(13):2789-2802.
31. Aoki Y, Hashizume R, Ozawa T, et al. An experimental xenograft mouse model of diffuse pontine glioma designed for therapeutic testing. *J Neurooncol*. 2012;108(1):29-35.
32. Hashizume R, Andor N, Ihara Y, et al. Pharmacologic inhibition of histone demethylation as a therapy for pediatric brainstem glioma. *Nat Med*. 2014;20(12):1394-1396.
33. Balyasnikova IV, Prasol MS, Ferguson SD, et al. Intranasal delivery of mesenchymal stem cells significantly extends survival of irradiated mice with experimental brain tumors. *Mol Ther*. 2014;22(1):140-148.
34. Dey M, Yu D, Kanojia D, et al. Intranasal oncolytic virotherapy with CXCR4-enhanced stem cells extends survival in mouse model of glioma. *Stem Cell Reports*. 2016;7(3):471-482.
35. Mangraviti A, Tzeng SY, Gullotti D, et al. Non-virally engineered human adipose mesenchymal stem cells produce BMP4, target brain tumors, and extend survival. *Biomaterials*. 2016;100:53-66.
36. Altanerova U, Benejova K, Altanerova V, et al. Dental pulp mesenchymal stem/stromal cells labeled with iron sucrose release exosomes and cells applied intra-nasally migrate to intracerebral glioblastoma. *Neoplasma*. 2016;63(6):925-933.
37. Clavreul A, Pourbaghi-Masouleh M, Roger E, Lautram N, Montero-Menei CN, Menei P. Human mesenchymal stromal cells as cellular drug-delivery vectors for glioblastoma therapy: a good deal? *J Exp Clin Cancer Res*. 2017;36(1):135.
38. Chastkofsky MI, Pituch KC, Katagi H, et al. Mesenchymal stem cells successfully deliver oncolytic virotherapy to diffuse intrinsic pontine glioma. *Clin Cancer Res*. 2021;27(6):1766-1777.
39. Bazak R, Houri M, El Achy S, Kamel S, Refaat T. Cancer active targeting by nanoparticles: a comprehensive review of literature. *J Cancer Res Clin Oncol*. 2015;141(5):769-784.
40. Johnson NJ, Hanson LR, Frey WH II. Trigeminal pathways deliver a low molecular weight drug from the nose to the brain and orofacial structures. *Mol Pharm*. 2010;7(3):884-893.
41. Hanson LR, Fine JM, Hoekman JD, et al. Intranasal delivery of growth differentiation factor 5 to the central nervous system. *Drug Deliv*. 2012;19(3):149-154.
42. Dhuria SV, Hanson LR, Frey WH II. Novel vasoconstrictor formulation to enhance intranasal targeting of neuropeptide therapeutics to the central nervous system. *J Pharmacol Exp Ther*. 2009;328(1):312-320.
43. Tafaghodi M, Jaafari MR, Sajadi Tabassi SA. Nasal immunization studies using liposomes loaded with tetanus toxoid and CpG-ODN. *Eur J Pharm Biopharm*. 2006;64(2):138-145.
44. Chen M, Li XR, Zhou YX, et al. Improved absorption of salmon calcitonin by ultraflexible liposomes through intranasal delivery. *Peptides*. 2009;30(7):1288-1295.

Disclosures

The authors report no conflict of interest concerning the materials or methods used in this study or the findings specified in this paper.

Brought to you by CCSS/BINASSS - DEPARTMENTO ADQ | Unauthenticated | Downloaded 06/19/23 04:42 PM UTC

Author Contributions

Conception and design: Hashizume, Sasaki, Watanabe, Frey, Zhang. Acquisition of data: Sasaki, Watanabe, He, Katagi, Suri, Ishi, Abe, Zhang. Analysis and interpretation of data: Hashizume, Sasaki, Watanabe, He, Katagi, Suri, Ishi, Abe, Zhang. Drafting the article: Hashizume, Sasaki, Watanabe, Frey, Zhang. Critically revising the article: Hashizume, Watanabe, Natsumeda, Frey, Zhang. Reviewed submitted version of manuscript: Hashizume, Sasaki, Watanabe, Natsumeda, Frey, Zhang. Approved the final version of the manuscript on behalf of all authors: Hashizume. Statistical analysis: Hashizume. Administrative/technical/material support: He. Study supervision: Hashizume, Natsumeda, Frey.

Supplemental Information

Online-Only Content

Supplemental material is available with the online version of the article.

Supplementary Figures S1 and S2. https://thejns.org/doi/suppl/10.3171/2022.9.JNS22715.

Correspondence

Rintaro Hashizume: Northwestern University Feinberg School of Medicine, Chicago, IL. rintaro.hashizume@northwestern.edu.

Brought to you by CCSS/BINASSS - DEPARTMENTO ADQ | Unauthenticated | Downloaded 06/19/23 04:42 PM UTC